Clinical Research on Foot & Ankle
ISSN: 2329-910X
Cifuentes-De la Portilla C et al., Clin Res Foot Ankle 2021, 9:5
Research Article
Open Access

Stress Concentrations caused by Lapidus Arthrodesis: A Finite Element Study

Pasapula C[1], Cifuentes-De la Portilla C[2*], Borja Gutierrez-Navarte[3], Larrainzar-Garijo R[3] and Bayod J[4]

[1]*Department of Orthopedics, University Queen Elizabeth Hospital, Kings Lynn, United Kingdom*
[2]*Department of Biomedical Engineering, University of Los Andes, Bogota, Colombia*
[3]*Department of Orthopaedics and Trauma, University Hospital Infanta Leonor, Madrid, Spain*
[4]*Department of Applied Mechanics and Bioengineering, University of Zaragoza, Spain*

Abstract

Lapidus arthrodesis is used in the treatment of hallux valgus, first ray instability and midfoot arthritis. Despite being commonly performed, few studies have addressed the regional biomechanical implications of this procedure. Our objective was to analyse the stress concentrations caused by two commonly performed Lapidus arthrodesis on surrounding bone and soft tissue structures of the foot. A finite element model was used to simulate the normal intact foot and scenarios of tissues deficiencies that are often associated when a Lapidus arthrodesis is performed. Our model includes all the foot bones, cartilage and major tendons and ligaments that support the foot arch. Both tensile stress and compressive forces were measured in the midfoot bones, joints and tibialis posterior tendon. Results showed that the classical Lapidus arthrodesis is associated with an increase of about 76% in the compressive stress generated around the first and second cuneiform joint, while the isolated metatarsocuneiform arthrodesis showed a non-significant increase in stress in this region. The Lapidus procedures slightly offload tensile stresses in the tibialis posterior tendon but were not alone able to compensate for the lack of a calcaneonavicular (spring) ligament failure despite increasing the rigidity of the arch. We concluded that the Lapidus arthrodesis does have regional implications on soft tissues and bone that are difficult to define. Whilst helping to decrease stresses in the tibialis posterior tendon Lapidus arthrodesis' allow correction of both deformity and instability in the first ray, however, they cannot compensate for the restoration of proximal talonavicular laxity/spring ligament strain when restoring arch integrity.

Keywords: Biomechanics; Flatfoot; Finite element modelling; Hallux valgus; Lapidus

Introduction

In the 1930's, Paul Lapidus described the surgical correction of the hallux abducto-valgus deformity using the first metatarsocuneiform joint arthrodesis [1]. The Lapidus procedure is a common operation performed to address the first ray in hallux valgus deformity and acquired metatarsal instability [2]. The latter is commonly done as an adjunct to other procedures in the correction of the planovalgus foot. In hallux valgus, surgery it is reserved for high intermetatarsal angle (IMA), hypermobile and arthritic first ray surgery [3]. In adult acquired flatfoot surgery, it can be used to address the first ray instability [2]. The classical Lapidus further addresses intercuneiform joint instability (first and second cuneiform) via fixation between the medial and middle columns. In the modified Lapidus procedure, only the metatarsocuneiform joint is fused [1]. While it is simpler, it does not address intercuneiform joint instability. Both Lapidus procedures can correct deformity, address midfoot instability and stabilize the metatarsocuneiform joint, using plates, screws or semi rigid constructs [4]. Although, the Lapidus is a well-known procedure, the biomechanical side effects that can arise in the foot have not been evaluated. Thus, these effects are not known despite its widespread use. This may be because studies that evaluate stresses are difficult to perform using clinical or cadaver evaluation. Some studies have evaluated the biomechanical effects of Lapidus procedures [5-8], but their evaluation is mainly structural. Difficulties arise in measuring the biomechanics of the inner foot (such as tissue stress distributions), standardizing different scenarios, and reproducing results from differences in foot geometries and tissues [9-11]. Internal tissue stresses and regional stress arising from both Lapidus arthrodesis are difficult more to establish. Additionally, cadaveric studies require expensive measurement equipment and meticulous control of tested tissues to guarantee their biomechanical characteristics. Thus, it is extremely difficult to obtain isolated information about each tissue with consistent results.

Finite element modelling (FEM) offers an alternative to this when studying the biomechanics of the human body. Many models have been used to evaluate foot biomechanics and the effects of surgical procedures. However, these models focus specifically on foot structure deformation and plantar pressure measurement [9,12]. This study aims to use a foot model to evaluate how two Lapidus arthrodesis procedures affect stresses on local joints and tissues. The finite element model includes all foot bones, cartilages, and main soft tissues that support the plantar arch. Evaluations of these arthrodeses were performed in the healthy state (with all the soft tissues intact) and simulating some soft tissue failures.

Materials and Methods

FE model description

Our model reconstructs an unloaded human foot of a 49 year old man with a weight of 75 Kg. The reconstructions are based on CT images and were performed using MIMICS V.10 (Materialize, Leuven, Belgium) [13-15]. The model includes bones (cortical and trabecular), plantar fascia, tibialis posterior tendon (TPT), Achilles tendon, flexor

***Corresponding author:** Christian Cifuentes-De la Portilla, Department of Biomedical Engineering, University of Los Andes, Bogota, Colombia, E-mail: cc.cifuentes@uniandes.edu.co

Received: May 10, 2021; **Accepted:** May 24, 2021; **Published:** May 31, 2021

hallucis longus (FHL), flexor digitorum longus (FDL), both peroneal tendons (Brevis and Longus) and cartilages. Due to the difficulty of segmenting the spring ligament and both plantar ligaments (short and long) from CT images, these tissues were reconstructed based on their anatomy, using body atlas and surgeons' guidance. A statement on ethical approval by a committee is not required for this work, because neither intervention nor any contact was made with the volunteer whose foot was used for reconstruction and modelling. However, we have the informed consent signed by this person accepting the use of their images to be used for foot modelling. This model has been already used to analyse the adult acquired flatfoot development [13-15]. The complete FE model is shown in Figure 1.

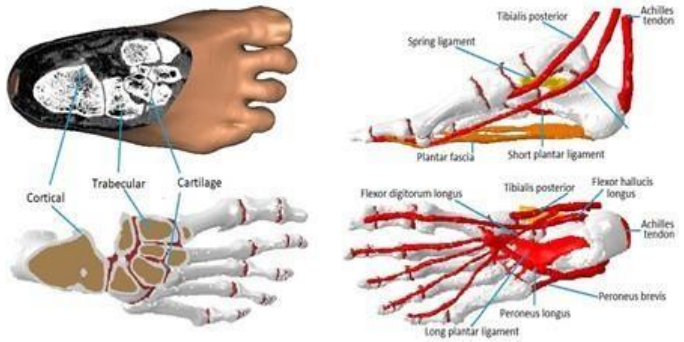

Figure 1: Detailed description of the FE model.

Meshing of the model

The meshing of the model was performed using ICEM CFD V.15 (Canonsburg, Pennsylvania, United States), generating 28 cortical bone pieces, 24 trabecular bone pieces, 26 cartilage segments, 6 tendons, 3 ligaments and the plantar fascia. To optimize the mesh size of each segment and check the mesh quality, a trial error approach was employed, following the recommendations of Burkhart [16]. They stated that to obtain reliable results, the total number of inaccurate elements must be less than 5%. The following conditions were considered in order to achieve a reasonable mesh size without compromising the calculation time: a minimum mesh size sufficiently small to fit into the tightest segments, a maximum mesh size consistent with the minimum, avoidance of large differences in element size between regions, a mesh accuracy of more than 99% of the elements being better than 0.2 mesh quality (Jacobians) and checking that the poor elements were located away from the region of greatest interest (Hindfoot bones, metatarsals, PF and SL). The equilibrium was found with 265,547 linear tetrahedral elements (C3D4). All parameters were within good mesh quality ratios (Table 1). Both finite element analysis and simulations were conducted with Abaqus/CAE 6.14-1 (Dassault Systémes, Vélizy-Villacoublay, France) using the available nonlinear geometry solver.

Quality metric	(Assessment criteria)	Accurate elements	Inaccurate elements
Element Jacobians	>0.2	99.2%	0.8%
Aspect ratio	<3	95.5%	4.5%
Min. angles	>30	97.6%	2.4%
Max. angles	>120	98.7%	1.3%

Table 1: Mesh quality metrics based on Burkhart et al. (2013) recommendations.

Biomechanical properties of model tissues

Tissue properties (Young's modulus and Poisson's ratio) of cortical bone, trabecular bone, ligaments and plantar fascia were assigned in accordance with published data: Cortical bone (E=17000 MPa, v=0.3), trabecular bone (E=700 MPa, v=0.3), ligaments (E=250 MPa, v=0.28) and Plantar fascia (E=240 MPa, v=0.28) [13]. Tendons and cartilage were modelled based on the Ogden model (hyperelastic material), using parameters previously reported in the literature [17-19].

The stress and compressive forces in the midfoot joints for the classical Lapidus and the modified Lapidus were evaluated. Simulated fusions were performed with a complete union of the cuneiform metatarsal joint (CM) and union between the first and second cuneiforms (Figure 2) by replacing the joint cartilage with cortical bone tissue. Fixation elements such as plates or screws were not included, because a complete joint fusion was simulated.

Figure 2: Explanation of how the arthrodesis was simulated. The cartilage material was replaced by a cortical bone in each of the fused joints.

Loading and boundary conditions

A simulated load was applied in the vertical direction and at 10 degrees of inclination. The distribution was as follows: Tibiotalar load transmission was set at 90% and Fibula Talus load transmission at 10% [14,15]. Tendon traction forces were included as described by [20]. To simulate ground contact, all simulations were performed by maintaining fixed nodes in the lower part of the calcaneus and blocking vertical displacement (z-axis) of the lower nodes of the first and fifth metatarsals (Figure 3) [13].

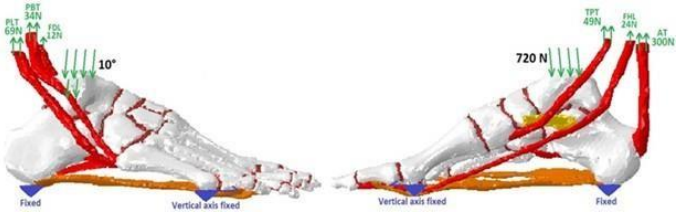

Figure 3: Boundary and loading settings applied to the foot model

Model validation

The model used in this analysis has been validated by other studies in relation to adult acquired flatfoot deformity [13]. These studies measured the vertical displacement of anatomical points in two different loading conditions: light loading and normal stance loading. Both were measured in the sagittal plane. This validation method compares the results obtained from the model against the average of values measured from real lateral RX images [21].

Model analysis and evaluation criteria

The biomechanical stress and compressive forces were quantified using the field output spectrum available in Abaqus/CAE. The parameters used for evaluation were both the Stress maximum principal (S. Max) and the Stress minimum principal (S. Min). These eigenvalues, which are generated in foot tissues during normal simulated stance, are closely related to the tensile stresses and compressive forces, respectively.

Results

Compressive forces in midfoot joints

This first analysis aimed to evaluate the differences in compressive forces within midfoot joints. Minimum principal stress was calculated in scenarios of intact and dysfunctional spring ligament. Simulations were performed in the reference case (without Lapidus) and in the presence of both Lapidus cases. The results are shown in Figure 4. All color scale values are in MPa (N/mm2). Red values depict less compressive forces, while blue values depict the highest forces. All the stress values were normalized to -20 MPa. The region marked shows the largest difference between the classical Lapidus and the modified Lapidus.

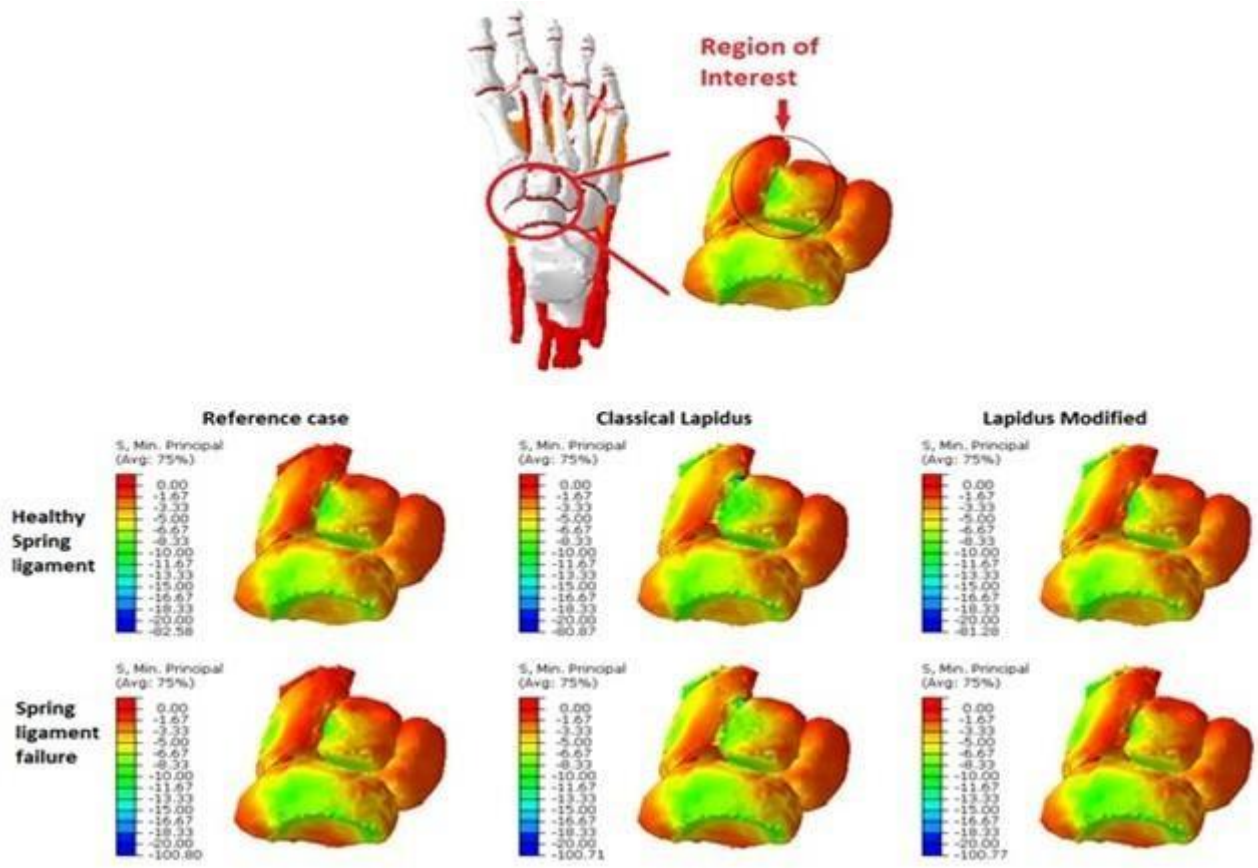

Figure 4: Compressive forces (Minimum principal stress in MPa) generated in the midfoot, including the navicular and cuneiform bones and cartilages.

Spring ligament failure increases stress generated in the first cuneiform representing the region of the insertion of the tibialis posterior tendon. With spring ligament insufficiency, our simulations do not show significant differences in the highest values between the two Lapidus arthrodesis procedures (Figure 4).

Compressive forces in the joint of the first and second cuneiform bones

To analyse and determine differential forces generated by both Lapidus arthrodesis procedures in regional joints such as the first/second intercuneiform joints and the naviculocuneiform joints, compressive forces were calculated by analysis of the cartilage section only. Analysis of the scenarios described above was included. The results are shown in Figure 5. As was commented in the previous section, the stress values were normalized to -20 MPa. The classical Lapidus generates a compressive force increase of 76% compared to the reference case. Additionally, the results show that the Lapidus arthrodeses were not able to prevent the notable increase in compressive force on the talonavicular joint (from yellow to orange in the color scale) when the spring ligament fails. This reinforces the importance of the spring ligament in the maintenance of the plantar arch for which distal stabilization would not be able to compensate.

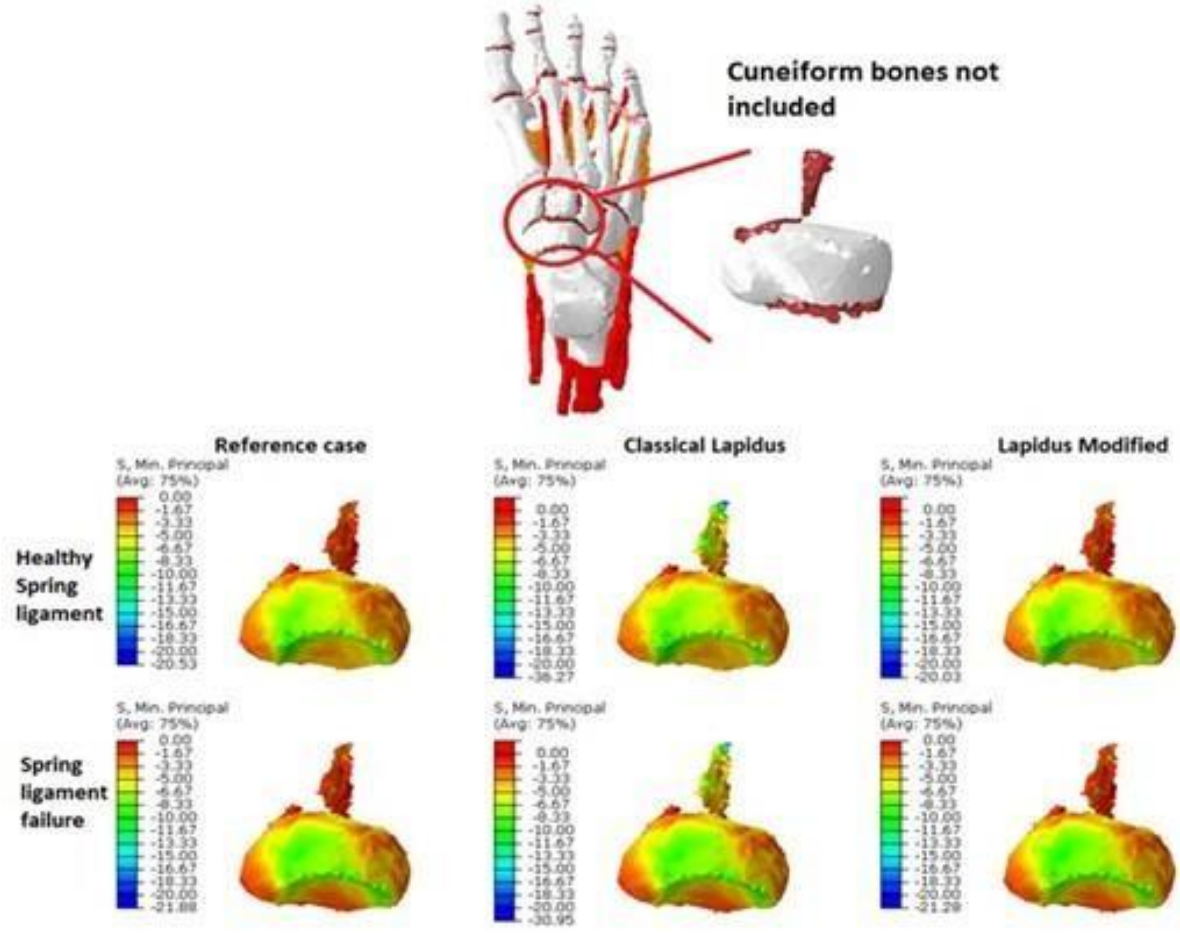

Figure 5: Compressive forces (Minimum principal stress in MPa) generated in the union cartilage of the first and second cuneiform and in the Navicular bone.

Bar charts were used to demonstrate results including the highest compressive forces obtained in all simulation scenarios (Figure 6).

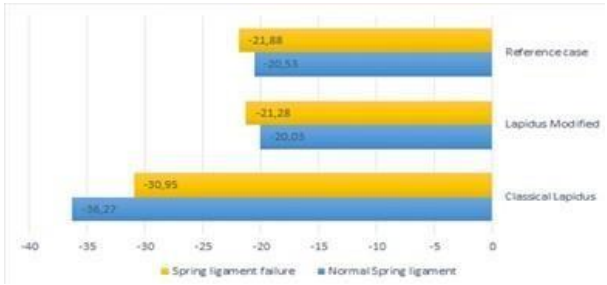

Figure 6: Comparison of the highest values of compressive forces generated in all simulated cases.

Biomechanical stress comparison traction forces

The spring ligament and the plantar fascia are the static stabilizers of the plantar arch [14,15]. The tibialis posterior tendon is the main dynamic stabilizer of the arch. We evaluated traction forces generated at the insertion area on the first cuneiform bone of the tibialis posterior tendon for both Lapidus types. The results are shown in Figure 7. The maximum principal stresses were measured. The color scale was normalized to 20 MPa. In this diagram, the blue scale represents the lowest stress values, whilst the red represents the highest. Neither of the Lapidus procedures evaluated had a significant effect on the traction forces at the insertion region of the tibialis posterior tendon. However, in the presence of spring ligament failure there was a significant increase in traction forces in the tibialis posterior despite the presence of additional stabilization of the first ray from both types of Lapidus procedure. The modified Lapidus arthrodesis generated a 79% increase in traction force.

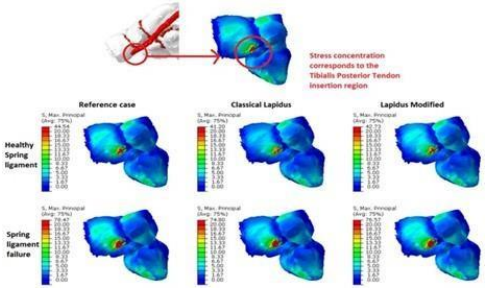

Figure 7: Traction forces (maximum principal stress in MPa) generated in midfoot bones. The region of insertion of the tibialis posterior

tendon is highlighted.

Maximum stress values generated for each scenario have been presented as bar graphs (Figure 8).

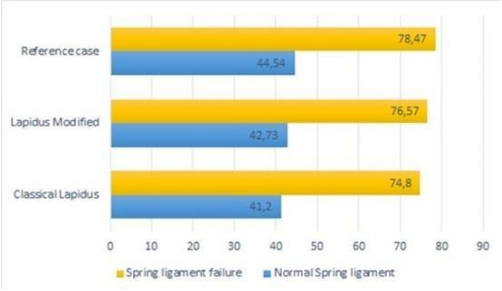

Figure 8: Comparison of the highest values of traction forces generated in all the cases simulated.

Discussion

Finite element analysis provides a useful means of understanding the effects of Lapidus arthrodesis on the surrounding tissues and how they behave as a result of these procedures. Few experimental studies have measured the comparative biomechanical effects of the Lapidus arthrodesis because of the difficulty of objectively measuring these parameters in cadavers. It is well known that a stable first ray prevents secondary issues such as metatarsophalangeal joint impingement and osteoarthritis. Stability prevents middle column overload resulting in second metatarsophalangeal joint synovitis, hammering, metatarsal hypertrophy/stress fractures, and tarsometatarsal degeneration [22]. A stable first ray provides a ground reaction force that helps resist pronation forces. Stability allows the transmission of compressive forces through the medial column to the hindfoot in the stance phase (60% of the gait cycle) [23].

Metatarsocuneiform instability can arise in hallux valgus from the medial displacement of the first metatarsal out of its soft tissue envelop which thus fails to restrain it in the dorsoplantar direction. Dorsoplantar instability can be marked in high intermetatarsal angle (IMA) hallux valgus. Clinical and cadaver studies have shown that first ray instability can also be driven by spring ligament insufficiency [24] even with a normal first intermetatarsal angle. These factors can both act concomitantly to increase first ray instability [24,25]. Addressing both may be important when considering treatment for instability.

Stabilization in hallux valgus can be achieved by osteotomies or fusion of the first cuneometatarsal (CM) joint with a Lapidus procedure. Proximal metatarsal osteotomies reduce the metatarsal head over the sesamoids and this realignment increases first ray stability and improves the windlass mechanism. However, recurrence of the instability may occur if spring ligament integrity is not addressed. Lapidus arthrodesis prevents this and can correct metatarsal pronation that osteotomes fail to address [26]. These procedures are commonly performed in high IMA hallux valgus and hypermobile CM joint to address degenerative changes. In flatfoot surgery, Lapidus arthrodesis decreases instability and addresses fixed dorsiflexion/supination. It can also be used as a substitute for opening wedge osteotomies [1,2].

The classical Lapidus procedure controls the intercuneiform pronation and coronal plane instability [27]. In our model, we created a rigid fusion between the middle and medial intercuneiform joints by changing joint tissue to bone. Surgically, this is achieved using many types of constructs from a screw fixation into the second metatarsal base or middle cuneiform to semi rigid fixation devices such as the mini tightrope [3].

The CM joint allows five degrees of dorsoplantar motion [28] which the Lapidus arthrodesis decreases. This has a clinical impact on foot shock absorption. The effects of first ray stabilization on the surrounding bone, joints, ligament, and tendons are not defined. Both Lapidus arthrodeses in our simulations do not lead to a significant increase in stress on the adjacent naviculocuneiform joint. Clinically, this is important as it is unlikely to accelerate degenerative changes in the naviculocuneiform joint.

In the classical Lapidus, there is a concentration of stress forces in the intercuneiform area around the fusion region. This local stress concentration within the bone is exacerbated when the spring ligament is also failed. Often this cause of instability is overlooked or not assessed for. Compressive forces through the second metatarsocuneiform joint increase in classical Lapidus arthrodesis. A coronal cross section of the intercuneiform region may explain the increased stress. In the stance phase, an upward ground reaction force through the stable first ray is transmitted to this region. The triangular shape of the cuneiform orientates this second metatarsocuneiform horizontally, that may create vertical vector compression force here. Differential load going through the second and the first ray that may also concentrates stress forces here. When the spring ligament is also lax, stress concentration increases from 20 MPa to 36 MPa, representing a 75% increase.

Hindfoot pronation may further accentuate the horizontal plane of the second metatarsal cuneiform joint as the medial pronates and further increases pressures. There was no significant increase in stress concentration through individual naviculocuneiform joint facets. The clinical significance of this stress localization to the midfoot is not certain. Elevated forces in the bone may lead to pain/bone edema/ stress features. This may be a cause of persistent pain in the foot. Caution with offloading during the union process may also allow the arthrodesis to form better. Both Lapidus arthrodesis leads to a small decrease in stress in the tibialis posterior regardless of the state of the spring ligament. The presence of a fused first metatarsocuneiform joint increases arch stiffness and exerts a greater ground reaction force through the more rigid medial column (a supination moment). This, therefore, decreases tensile stresses in the tibialis posterior tendon. Spring ligament deficiency significantly increases the traction forces in the tibialis posterior that further stability in the first ray can only partially counteract. Lapidus arthrodesis used to treat first ray instability in the presence of spring ligament insufficiency only leads to a small decrease in the traction forces in the tibialis posterior [2]. This is important clinically as when correcting both hallux valgus and first ray instability to treat second ray overload pathology, stabilizing the first ray alone will not offload the tibialis posterior tendon if it has become reactive and symptomatic unless the spring ligament laxity is corrected. Further offloading of the talonavicular axis would be needed by spring ligament augmentation or a calcaneal osteotomy.

Conclusion

We conclude that computational modelling provides a useful insight into the regional effects of Lapidus arthrodesis on local tissues/joints, helping to evaluate them in ways not achievable by cadaver modelling. The Lapidus arthrodesis is such a commonly used procedure to address both instability and deformity of the first

ray that even small changes in regional effects on tissues need to be understood. Each arthrodesis has regional effects on other structures including the tibialis posterior tendon, spring ligament, and bone stress within the bones themselves. The widespread usage of these operations means that this increased understanding is beneficial.

This study has some limitations, which include the lack of an evaluation of fixation devices such as screws, plates, and bone graft. However, it does not affect the joint and tissue stress evaluation performed nor the clinical interpretation of the results. Additionally, we accept that Lapidus arthrodesis may result in the shortening of the hallux from cuts required to correct the deformity. This shortening was not considered in the model, because joint fusion was simulated replacing the cartilage by cortical bone.

Acknowledgement

The authors gratefully acknowledge the support of the Ministry of Economy and Competitiveness of the Government of Spain through the project PID2019-108009RB-I00.

Author Disclosure Statement

The authors declare that they have no competing financial interests.

References

1. Mote G, Yarmel D, Treaster A (2009) First metatarsal cuneiform arthrodesis for the treatment of first ray pathology. J Foot Ankle Surg 48: 593-601.
2. Thompson IM (2005) Fusion rate of first tarsometatarsal arthrodesis in the modified Lapidus procedure and flatfoot reconstruction. Foot Ankle Int 26: 698-703.
3. Ellington JK, Myerson MS, Coetzee JC, Stone RM (2011) The use of the Lapidus procedure for recurrent hallux valgus. Foot Ankle Int 32: 674-80.
4. King CM (2015) Modified Lapidus arthrodesis with crossed screw fixation: early weight bearing in 136 patients. J Foot Ankle Surg 54: 69-75.
5. Bierman RA, Christensen JC, Johnson CH (2001) Biomechanics of the first ray. Part III. Consequences of Lapidus arthrodesis on peroneus longus function: A three dimensional kinematic analysis in a cadaver model. J Foot Ankle Surg 40: 125-131.
6. Cottom J, Baker JS (2016) Comparison of locking plate with interfragmentary screw versus plantarly applied anatomic locking plate for Lapidus arthrodesis: a biomechanical cadaveric study. Foot Ankle Spec 10: 227-231.
7. Garas PK, Disegna ST, Patel AR (2018) Plate alone versus plate and lag screw for Lapidus arthrodesis: A biomechanical comparison of compression Foot Ankle Spec 11: 534-538.
8. Drummond D, Motley T, Kosmopoulos V, Ernst J (2018) Stability of locking plate and compression screws for Lapidus arthrodesis: a biomechanical comparison of plate position. J Foot Ankle Surg 57: 466-470.
9. Wang Z, Kido M, Imai K, Ikoma K, HiraiS (2016) Study of surgical simulation of flatfoot using a finite element model. In Innovation in Medicine and Healthcare, 353-363.
10. Wang Y, Wong DWC, Zhang M (2016) Computational models of the foot and ankle for pathomechanics and clinical applications: a review. Ann Biomed Eng 44: 213-221
11. Wong DWC, Wang Y, Leung AKL, Yang M, Zhang M (2018). Finite element simulation on posterior tibial tendinopathy: Load transfer alteration and implications to the onset of pes planus. Clin Biomech (Bristol, Avon) 51: 10-16.
12. Wang Z, Kido M, Imai K, Ikoma K, Hirai S (2018) Towards patient specific medializing calcaneal osteotomy for adult flatfoot: A finite element study. Comp methods in biomech biomed eng 21: 332-343.
13. Cifuentes-De la Portilla C, Larrainzar-Garijo R, Bayod J (2018) Biomechanical stress analysis of the main soft tissues associated with the development of adult acquired flatfoot deformity. Clin Biomech (Bristol, Avon) 61: 163-171.
14. Cifuentes-De la Portilla C, Larrainzar-Garijo R, Bayod J (2019) Analysis of biomechanical stresses caused by hindfoot joint arthrodesis in the treatment of adult acquired flatfoot deformity: A finite element study. Foot Ankle Surg 26: 412-420.
15. Cifuentes-De la Portilla C, Larrainzar-Garijo R, Bayod J (2019) Analysis of the main passive soft tissues associated with adult acquired flatfoot deformity development: A computational modelling approach. J Biomech 84: 183-190.
16. Burkhart TA, Andrews DM, Dunning CE (2013) Finite element modelling mesh quality, energy balance and validation methods: A review with recommendations associated with the modelling of bone tissue. J Biomech 46: 1477-1488.
17. Garcia-Aznar JM, Bayod J, Rosas A, Larrainzar R, García-Bógalo R, et al. (2009) Load transfer mechanism for different metatarsal geometries: A finite element study. J Biomech Eng 131: 021011(1-7).
18. Mansour JM (2003) Biomechanics of cartilage. Kinesiology: the mechanics and pathomechanics of human movement 2: 66-79.
19. Wu L (2007) Non-linear finite element analysis formusculoskeletal biomechanics of medial and lateral plantar longitudinal arch of Virtual Chinese Human after plantar ligamentous structure failures. Clin Biomech (Bristol, Avon) 22: 221-229.
20. Arangio GA, Salathe EP (2009) A biomechanical analysis of posterior tibial tendon dysfunction, medial displacement calcaneal osteotomy and flexor digitorum longus transfer in adult acquired flat foot. Clin Biomech (Bristol, Avon) 24: 385-390.
21. Tao K, Ji WT, Wang DM, Wang CT, Wang X (2010) Relative contributions of plantar fascia and ligaments on the arch static stability: A finite element study. Biomed Tech 55: 265-271.
22. Morton JD (1928) Hypermobility of the first metatarsal bone: The interlinking factor between matarsalgia and longitudinal arch strains. J Bone Joint Surg Am 10: 187-196.
23. Doxey GE (1985) Management of Metatarsalgia with foot orthotics. J Orthop Sports Phys Ther 6: 324-333.
24. Chu IT, Myerson MS, Nyska M, Parks BG (2001) Experimental flatfoot model: the contribution of dynamic loading. Foot Ankle Int 22: 220-225.
25. Jesse DF, Coughlin MJ (2013) Hallux valgus and hypermobility

of the first ray: Facts and fiction. Int Orthop 37: 1655-1660.

26. Wagner P, Wagner E (2018) Is the rotational deformity important in our decision-making process for correction of hallux valgus deformity? Foot Ankle Clin 23: 205-217.

27. Kopp FJ, Patel MM, Levine DS, Deland JT (2005) The modified Lapidus procedure for hallux valgus: A clinical and radiographic analysis. Foot Ankle Int 26: 913-917.

28. Whittaker EC, Aubin PM, Ledoux WR (2011) Foot bone kinematics as measured in a cadaveric robotic gait simulator. Gait Posture 33: 645-650.